Progress In Electromagnetics Research M, Vol. 69, 161–170, 2018

A Compact Coupling Structure for Diplexers and Filtering Power Dividers

Yun Wu[1, 2], Ruiheng Wu[1], and Yi Wang[1, 3, *]

Abstract—This paper presents a compact and novel coupling structure for diplexers and power dividers based exclusively on coupled resonators. It consists of two cross-coupled structures joined together by two common resonators with a cluster of only four resonators. For a diplexer, it represents one of the most compact topologies that produces two 2nd-order channel filters with two fully controllable transmission zeros. This can be used to increase the rejection and isolations between channels without increasing the number of resonators. The same topology can also be used to realise a 3rd-order filtering power divider (FPD), with its embedded cascade trisection (CT) structure generating an asymmetric transmission zero. The coupling matrices of several diplexers and power dividers have been synthesized. Two microstrip diplexers with different positions of the transmission zeros have been demonstrated to verify the device concept. A 1.8 GHz FPD with a fractional bandwidth of 5% has also been prototyped, showing an improved out-of-band rejection from 15 dB to 25 dB below 1.71 GHz. The isolation performance of the divider has been investigated and improved from 7 dB to 18 dB across the band by adding only one resistor.

1. INTRODUCTION

Diplexers and multiplexers are of great importance in microwave applications as key passive components in many modern wireless systems such as mobile communication systems employing frequency division duplex (FDD). They are used for sharing a single antenna between a transmitter and a receiver or distributing signals to multiple channels. Many structures and circuit topologies have been developed for diplexers and multiplexers, using hybrid couplers, manifolds, T-junctions or all-resonator structures [1–4]. Among these, the all-resonator structures have been the focus of lots of recent work for their potentials in circuit miniaturization [4–6]. Such a structure also offered the possibilities for new topologies, such as a cascaded quadruplet (CQ) in the common stem of resonators as demonstrated in [4], which introduced transmission zeros in the guard band of diplexers.

All-resonator structures have also been used to design power dividers with integrated filtering functions — the so-called filtering power dividers (FPDs) [7–12]. Such a functional integration effectively reduces the component count and circuit footprint. Resonators and the couplings between them [13] replace the conventional transmission line sections used in many power dividers such as Wilkinson [14–16]. Synthesis methods for FPDs have also been developed [17, 18]. Isolation is an important performance parameter of a FPD to be considered in the design. Resistors were commonly used to improve matching at the output ports and therefore achieve good isolation but usually over a narrow frequency range [8]. Together with carefully placed resistors, coupling structures and stepped-impedance resonators (SIRs) have been reported to provide improved isolation over a wider bandwidth [19, 20].

Received 14 April 2018, Accepted 6 June 2018, Scheduled 15 June 2018

* Corresponding author: Yi Wang (y.wang.1@bham.ac.uk).

[1] Department of Engineering Science, University of Greenwich, Kent ME4 4TB, U.K. [2] National Laboratory for Superconductivity, Institute of Physics, Chinese Academy of Sciences, Beijing, China. [3] Department of Electronic, Electrical and System Engineering, University of Birmingham, B15 2TT, U.K.

In this paper, a compact coupling structure based on a four-resonator cluster is proposed for both diplexers and FPDs. It was inspired by a filtering power divider which applied two CQ structures to generate transmission zeros for selectivity improvement [9]. In the diplexer proposed here, each channel consists of one cascade-trisection-like (CT-like) structure [21], being configured to generate an asymmetric transmission zero on the opposite side of the guard band. The two CT-like structures are placed side-by-side and the coupling topology is designed so that two resonators are shared between the two channels. Although the proposed structure has one less reflection zero at each channel than a CT structure (two versus three zeros), it minimizes the required number of resonators while still achieving the prescribed transmission zeros. The same topology is then applied to a filtering power divider, where each branch of the divider was embedded with one cascade trisection (CT) structure, generating an asymmetric transmission zero on one side of the passband. Again, two resonators are shared between the two branches, reducing the required number of resonators to four, as compared with [22], while still achieving a 3rd-order filtering response with improved out-of-band rejection. An optimization-based synthesis method has been used to acquire the coupling matrices for the proposed diplexers and FPDs. The paper is organized as follows. The design is detailed in Section 2, starting with the diplexer topology, coupling matrix and EM simulation, and followed by the filtering power divider design based on the same topology. Section 3 reported the measurement results and conclusions are drawn in Section 4.

2. DESIGN

2.1. Diplexer Topology and Coupling Matrix

The topology of the proposed diplexer is shown in Fig. 1(a). Each circle denotes a resonator. The lines between them denote the electromagnetic coupling, where the dashed line represents an opposite sign of the coupling to the solid line. The two CT-like structures (resonators 1, 2, 4 and resonators 1, 3, 4) are embedded in the topology. Signal paths 1-4-2 and 1-4-3 correspond to the two channels, respectively. Resonators 1 and 4 are the common resonators shared between the two channels. Paths 1-2 and 1-3 provide the cross couplings in the two CT-like structures. For comparative illustration, Fig. 1(b) shows the topology of a conventional resonator-based diplexer without the cross couplings. The opposite signs of the couplings (resonators 2-4 and 3-4) in Fig. 1(a) are utilised to generate two asymmetric transmission zeros, one at a frequency above the lower band and the other below the higher band. The positions of the zeros can be adjusted, as will be demonstrated later, to control and improve the rejection and inter-channel isolation. This 3-port structure represents a very compact coupling structure that gives two 2nd-order channel filters and two transmission zeros. It is important to note that the number of achievable poles in the coupling structure does not exceed the number of resonators — four in this case. So, two poles (reflection zeros) can be expected from each channel. This structure is therefore not equivalent to two CT structures, which would contain six resonators (six poles).

To demonstrate the capability of the topology, a set of coupling matrices are synthesised for four diplexers with widely different positions of the transmission zeros. All of them are designed for two channels at 1.71–1.74 GHz and 1.85–1.89 GHz around the centre frequency f_0 of 1.8 GHz, with return

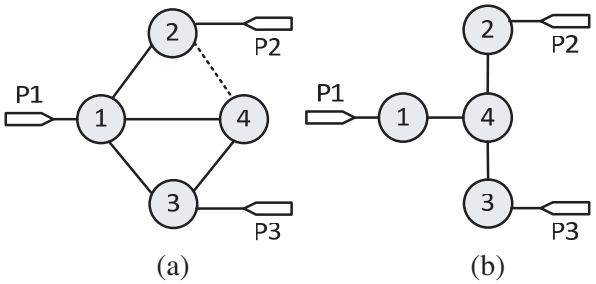

Figure 1. Coupling topologies. (a) The proposed diplexer, (b) a resonator-based diplexer without cross couplings.

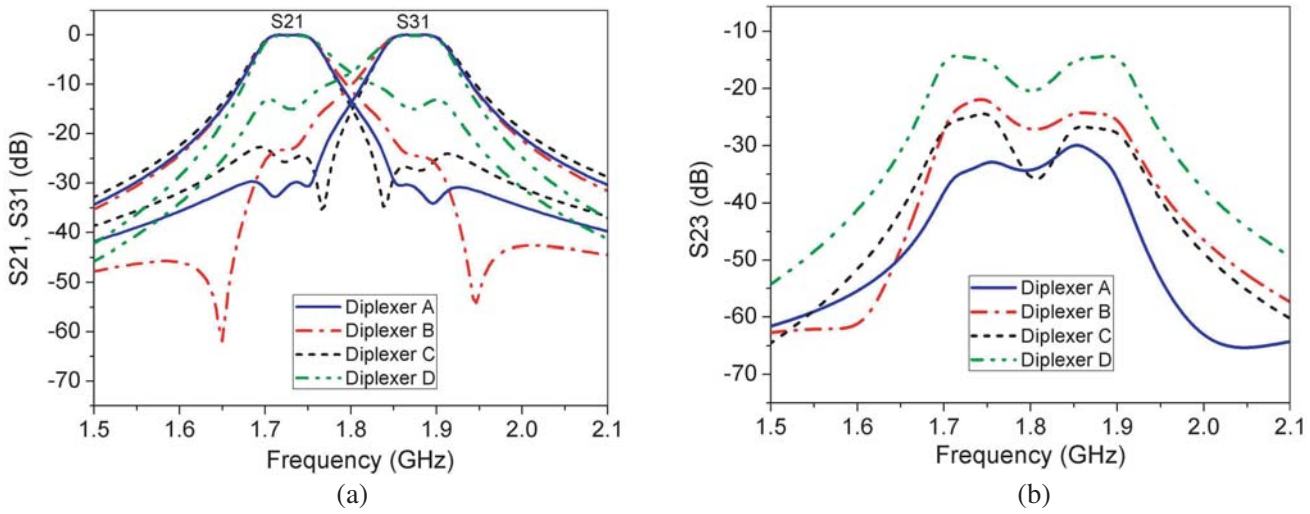

Figure 2. Calculated responses of four diplexers from the synthesised coupling matrices. (a) Transmission coefficients, (b) isolation between Port 2 and 3.

losses of 20 dB. As shown in Fig. 2, Diplexer-B exhibits its transmission zeros at 1.651/1.944 GHz, outside of the channel passbands. Diplexer-C has two zeros within the guard band at 1.767/1.838 GHz. As for Diplexer-A, two transmission zeros are designed to be inside the passband of the opposite channels at 1.72/1.88 GHz. Although they are not clearly identifiable, their effect on the improved rejection and isolation level (over 30 dB) is evident from Figs. 2(a) and (b). All three diplexers (A, B, and C) with the topology of Fig. 1(a) perform much better than Diplexer-D of the topology of Fig. 1(b).

The coupling matrices for the four diplexers are synthesised using an optimisation based method published and detailed in [4]. In this method, the expected S-parameters of the coupled-resonator network is determined by the coupling matrix through a so-called normalised matrix $[A]$, written as [23]:

$$[A] = [q] + p[U] - j[m] \tag{1}$$

where $[U]$ is the $N \times N$ identity matrix, $[m]$ the normalised coupling matrix, and $[q]$ a diagonal matrix with only $[q]_{ii} = 1/q_{e,i} \neq 0$. $q_{e,i}$ is the normalised external quality factor from the port attached to the i-th resonator and

$$p = j \cdot (f/f_0 - f_0/f)/\text{FBW} \tag{2}$$

where FBW is the fractional bandwidth, and f is the central frequency. In this diplexer design,

$$\text{FBW} = (f_h - f_l)/f_0, \quad f_0 = \sqrt{f_l \cdot f_h} \tag{3}$$

where $f_l = 1.71$ GHz and $f_h = 1.89$ GHz. The S-parameter of the diplexer can be written as

$$S_{nn} = \pm\left(1 - \frac{2}{q_{e,n}}[A]^{-1}_{nn}\right) \tag{4}$$

$$S_{mn|m\neq n} = \frac{2}{\sqrt{q_{e,n} \cdot q_{e,m}}}[A]^{-1}_{mn} \tag{5}$$

where S_{nn} is the refection coefficient from port P_n which is attached to the n-th resonator, and S_{mn} is the transmission coefficient from port P_n to P_m. In the real frequency domain, the external quality factors and the coupling matrix can be found by:

$$Q_{e,i} = q_{e,i}/\text{FBW}, \quad M_{i,j} = m_{i,j} \cdot \text{FBW} \tag{6}$$

Using the optimisation method [4], the de-normalised matrices for Diplexer-A and B are found to

be

$$[M]_A = \begin{bmatrix} 0 & 0.0212 & 0.0217 & 0.0854 \\ 0.0212 & -0.0818 & 0 & -0.0196 \\ 0.0217 & 0 & 0.0821 & 0.0188 \\ 0.0854 & -0.0196 & 0.0188 & 0 \end{bmatrix} \tag{7}$$

$$[M]_B = \begin{bmatrix} 0 & 0.036 & 0.0368 & 0.1453 \\ 0.036 & -0.139 & 0 & -0.0334 \\ 0.0368 & 0 & 0.1395 & 0.0319 \\ 0.1453 & -0.0334 & 0.0319 & 0 \end{bmatrix} \tag{8}$$

The matrix for Diplexer-D without the cross couplings is given by

$$[M]_D = \begin{bmatrix} 0 & 0 & 0 & 0.0891 \\ 0 & -0.0733 & 0 & -0.0394 \\ 0 & 0 & 0.0733 & 0.0394 \\ 0.0891 & -0.0394 & 0.0319 & 0 \end{bmatrix} \tag{9}$$

The external quality factors Q_e for the three ports of each diplexer are [19.17, 38.33, 38.41], [18.20, 36.69, 36.07] and [16.54, 36.62, 36.62], respectively. It can be seen from the matrices that the two common resonators (1 and 4) are tuned to f_0 in all diplexers, whereas resonator 2 resonates at below f_0 and the resonator 3 at above f_0. For Diplexer-A and B, the coupling coefficient $M_{2,4}$ and $M_{3,4}$ are opposite in signs so as to generate the asymmetric transmission zeros by the CT-like coupling structures.

2.2. EM Simulation of the Diplexers

To verify the controllable transmission zeros and therefore the rejection and inter-channel isolation as illustrated in Fig. 2, we have chosen to design and fabricate Diplexer-A and Diplexer-B as the demonstrators. These two topologies are also of more relevance to practical applications where channel isolation or out-of-band rejection are often concerned. Microstrip structures have been used to implement the circuits for its ease of fabrication, compact size and low cost. A Rogers RO4003C substrate with a dielectric constant of 3.55, a loss tangent of 0.0029 (nominal value at 10 GHz) and a thickness of 1.524 mm is selected for the design. Open loop resonators with a line width of 1 mm are used for the construction of the diplexer as they not only accommodate a compact layout, but also allow both positive and negative couplings to be realised. All simulations are performed in Sonnet 15.52.

The resonance frequency f_i of each asynchronously tuned resonator is found using the expression

$$f_i = \frac{f_0}{\sqrt{1 - M_{ii}}} \tag{10}$$

and the coupling coefficients between the asynchronously coupled resonators are calculated using the formula in [23].

The layout of Diplexer-A after optimisation is shown in Fig. 3. Dimensions of Diplexer-A and B are listed in the caption. It has been found from the phase responses (not shown here) that the coupling between resonator 2 and 4 is dominantly magnetic whereas the others are dominantly electric for both diplexers. The couplings between 1 and 3 and between 1 and 2 are the cross couplings in the CT-like structures. Stubs are added to the open-loop resonators to better control the couplings.

The simulated responses of Diplexer-A and B are shown in Fig. 4. Insertion losses in both diplexers are approximately 2.3 dB, and return losses are better than 20 dB in all channels. It can be found that the isolation of Diplexer-A is over 30 dB, higher than the 20 dB in Diplexer-B. This difference results from the different positions of the transmission zeros. The simulated S_{11} fits extremely well with the calculated responses from Fig. 2. However, a transmission zero at around 1.56 GHz appears in simulations for both diplexers. This is due to the tapped feedline on resonator 1 that causes a transmission notch. Current density simulation results have confirmed this point.

2.3. FPD Topology and Coupling Matrix

The same topology shown in Fig. 1(a) can be used to realise a 3rd-order two-way FPD. However, there are two main differences between the diplexer and the FPD. First, the couplings of the FPD are

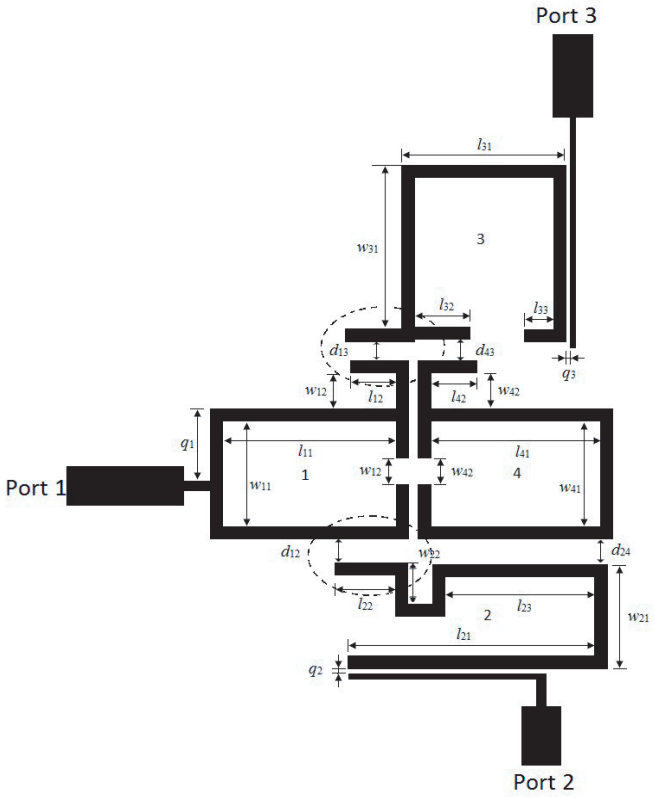

Figure 3. Layout of Diplexer-A. Dimensions in the figure are: $l_{11} = 14.2$, $l_{12} = 3.75$, $w_{11} = 8.65$, $w_{12} = 2.2$; $l_{21} = 20.15$, $l_{22} = 5.0$, $l_{23} = 12.25$, $w_{21} = 8.5$, $w_{22} = 3.35$; $l_{31} = 13.4$, $l_{32} = 4.55$, $l_{33} = 2.4$, $w_{31} = 13.45$; $l_{41} = 13.85$, $l_{42} = 3.75$, $w_{41} = 8.65$, $w_{42} = 2.2$; $d_{12} = 2.0$, $d_{13} = 1.6$, $d_{24} = 2.15$, $d_{43} = 1.75$, $d_{14} = 0.8$; $q_1 = 5.95$, $q_2 = 0.45$, $q_3 = 0.35$. For Diplexer-B, these dimensions are: $l_{11} = 14.0$, $l_{12} = 3.74$, $w_{11} = 8.64$, $w_{12} = 2.2$; $l_{21} = 19.96$, $l_{22} = 5.0$, $l_{23} = 12.2$, $w_{21} = 8.9$, $w_{22} = 2.14$; $l_{31} = 13.4$, $l_{32} = 4.54$, $l_{33} = 3.0$, $w_{31} = 10.84$; $l_{41} = 13.94$, $l_{42} = 3.74$, $w_{41} = 8.64$, $w_{42} = 2.2$; $d_{12} = 2.86$, $d_{13} = 3.6$, $d_{24} = 1.36$, $d_{43} = 1.0$, $d_{14} = 0.76$; $q_1 = 5.84$, $q_2 = 0.3$, $q_3 = 0.36$. Unit: mm.

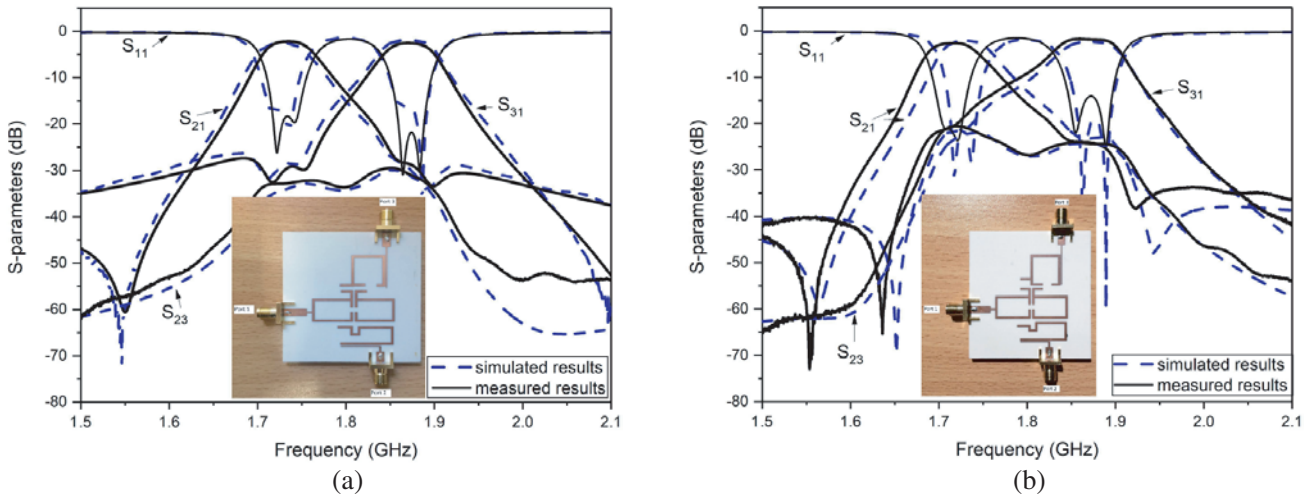

Figure 4. Measured responses of the diplexers as compared with simulations, with the insets showing the fabricated circuits. (a) Diplexer-A, (b) Diplexer-B.

symmetric with respect to the common resonators 1 and 4. Second, the coupling $M_{2,4}$ and $M_{3,4}$ are of the same sign and value. Due to symmetry, the four-resonator structure represents two CT structures (resonators 1, 2, 4 and resonators 1, 3, 4) embedded in the topology. Similar to the diplexers, the two main signal paths are 1-4-2 and 1-4-3. Paths 1-2 and 1-3 provide the cross couplings in the CT structures. The topology contains the minimum number of resonators required to realise the two-way 3rd-order filtering divider with one transmission zero.

The coupling matrix for the FPD is synthesised for a centre frequency of 1.8 GHz, a fractional bandwidth of 5%, a return loss of 20 dB and a transmission zero at 1.7 GHz. The de-normalised matrix $[M]$ is acquired using the optimisation based synthesis method [4] and given by

$$[M] = \begin{bmatrix} 0.00935 & 0.02755 & 0.02755 & 0.05555 \\ 0.02755 & 0.00935 & 0 & 0.0393 \\ 0.02755 & 0 & 0.00935 & 0.0393 \\ 0.05555 & 0.0393 & 0.0393 & -0.03685 \end{bmatrix} \tag{11}$$

and all three external quality factors at the ports are 13.556. It can be found that all four resonators are asynchronously tuned. The frequencies of resonators 1, 2 and 3 are the same and higher than f_0, whereas the frequency of resonator 4 is lower. All mutual coupling coefficients are positive, which indicates the same type of couplings between resonators. These relations in frequencies and couplings from the CT structure result in one transmission zero below the passband. The calculated response from the matrix is shown in Fig. 5. The transmission zero at 1.7 GHz can be seen. The out-of-band rejection below the passband has been improved to 25 dB as compared with the higher rejection band.

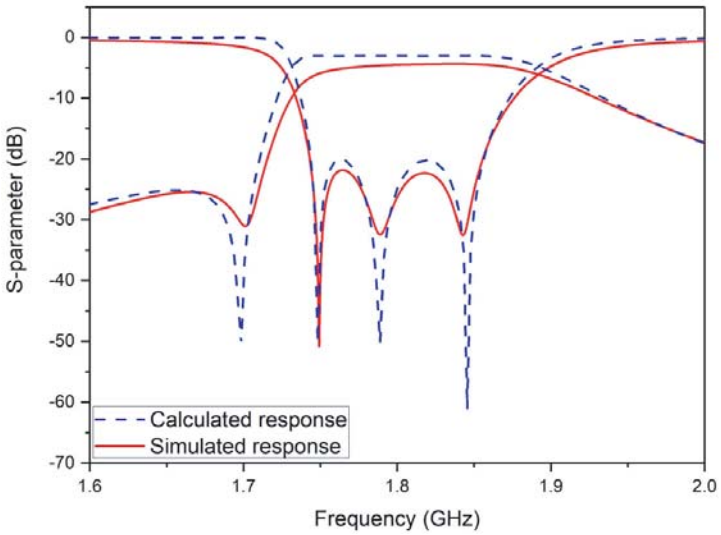

Figure 5. Calculated and simulated response of the proposed filtering power divider.

2.4. EM Simulation of the FPD

The same substrate is chosen for the FPD. In consideration of the symmetry of the device, modified full-wavelength open-loop resonators are used. Another reason to use full-wavelength resonators instead of quarter-wavelength resonators is to avoid drilling grounding holes on the substrate. The layout of the power divider after optimization is shown in Fig. 6. The inter-digital structures with a gap width of 1.5 mm ensure couplings between these resonators are electrical. The simulated responses are shown in Fig. 5. The return loss is better than 20 dB, and the insertion loss is 4.3 dB, higher than the calculation (lossless) due to the losses from the Rogers substrate. All the refection zeros and transmission zeros correspond very well with the calculated results.

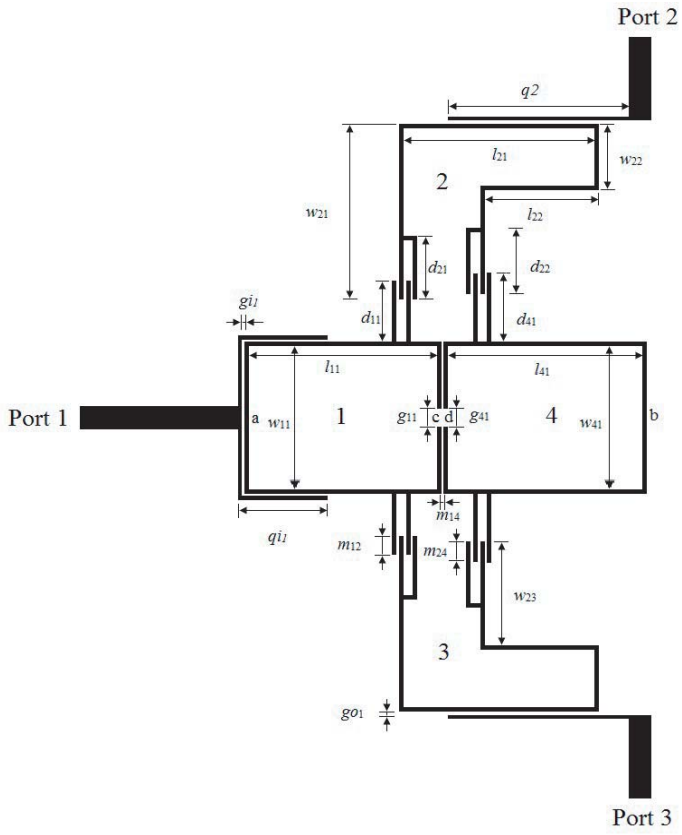

Figure 6. Layout of the power divider before adding the isolation resistor. The widths of the feedline are 3.2 mm, and widths of microstrip of resonators are 0.5 mm. The dimensions are: $qi_1 = 12.7$, $gi_1 = 0.5$, $l_{11} = 27.04$, $d_{11} = 8.9$, $w_{11} = w_{41} = 20.8$, $g_{11} = g_{41} = 2.8$, $l_{41} = 27.96$, $d_{41} = 10.06$, $l_{21} = 27.5$, $l_{22} = 16.36$, $w_{21} = 25.2$, $w_{22} = 9.4$, $w_{23} = 15.1$, $d_{21} = 9.0$, $d_{22} = 9.44$, $m_{12} = 2.6$, $m_{24} = 2.94$, $m_{14} = 0.4$, $q_2 = 25.8$, $go_1 = 0.64$. Unit: mm.

3. FABRICATION AND MEASUREMENTS

The diplexers and FPDs were fabricated using LPKF ProtoMat S63 micro-milling process, and the prototypes are shown in the insets of Fig. 4 and Fig. 7 respectively. The overall dimension of the diplexers is 55 mm × 60 mm, and the minimum gap used is 0.3 mm. For the FPD, this is 100 mm × 110 mm, and the minimum gap used is 0.4 mm.

The measurements were taken by Agilent N5230A network analyser. Shown in Fig. 4 are the measured results of the diplexers as compared with the simulations. Insertion losses in all channels are between 2.0 and 2.4 dB, and the return losses are better than 15 dB after tuning. In general, measurements and simulations agree very well with each other. There are small frequency shifts, for instance, in the lower band of Diplexer-B, which is caused by machining tolerance. Very importantly, it can be observed that the isolation between the two channels in Diplexer-B is 20 dB, whereas in Diplexer-A this is improved to 30 dB by the implementation of the transmission zeros, which correspond very well with the simulation results.

For the FPD, Fig. 8 shows the measured results in comparison with the simulation. The measured insertion loss is 4.2 dB, and the return loss is better than 19 dB after tuning, corresponding well with the simulated results. However, the measured bandwidth is wider, and the centre frequency is lower. As a result, the transmission zero shifts to a lower frequency. However, it still can be observed that the measured band edge is of the same shape as the simulated, and the out-of-band rejection has been improved to 25 dB. The discrepancy is attributed to fabrication tolerances which was not fully compensated for by tuning. It is noted that tuning was simply done by patching tiny dielectric bits

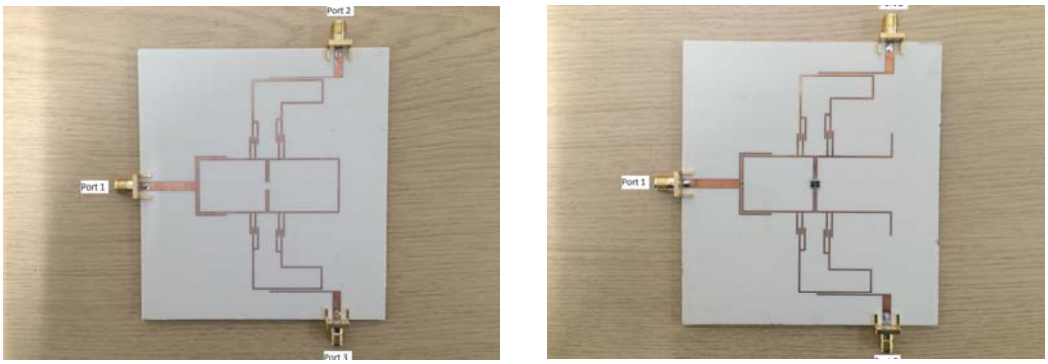

(a) (b)

Figure 7. Photograph of the fabricated FPDs. (a) The original FPD before adding the isolation resistor, (b) the FPD with the isolation resistor.

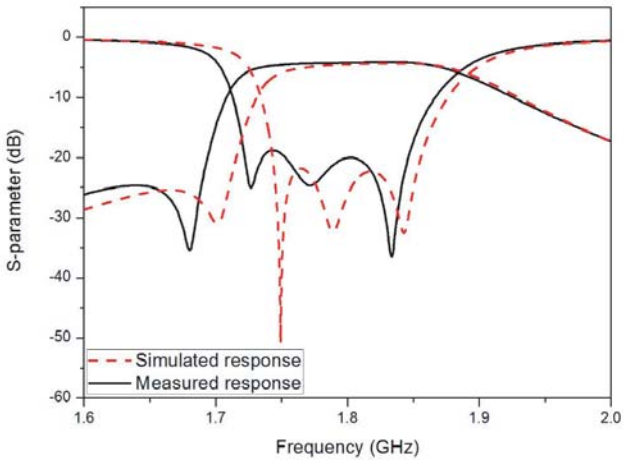

Figure 8. Measured and simulated responses of the proposed FPD without the isolation resistor.

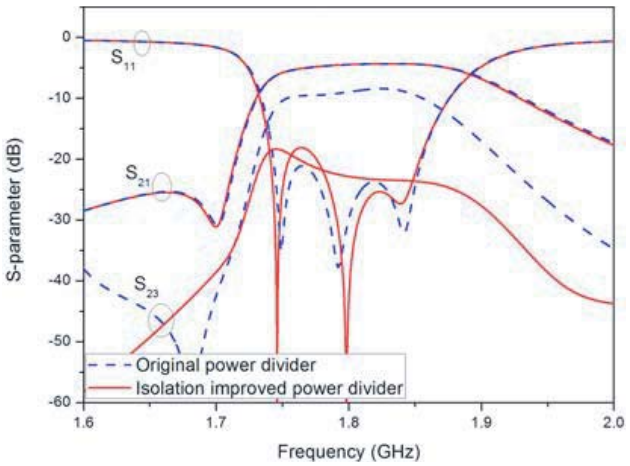

Figure 9. Comparison of the simulated transmission, reflection and isolation responses before and after adding the 75 Ω isolation resistor.

upon the microstrip lines in this work.

Now the in-band isolation of the proposed power divider is investigated. Typically, good isolation condition is only achievable at a particular frequency or over a narrow band [9]. In this work, by optimizing the position and value of only one resistor, the isolation of the proposed FPD can be improved across the passband.

Due to the symmetric structure of the proposed power divider and the use of full wavelength resonators, it is possible to split resonators 1 and 4 into separate halves at points a and d (marked out in Fig. 6) while keeping the impedance matching at the input and the transmission performance. This can also be explained using an even mode analysis. By adding a resistor across the gap at the position c (Fig. 6), the isolation in the modified power divider can be improved from 7 dB to 18 dB (Fig. 9) across the pass band, while keeping the reflection and transmission responses nearly unchanged. Optimization finds the resistor value is 75 Ω. The fabricated prototype of the isolation-improved FPD is shown in Fig. 7(b). It should be noted that different from resonator 4 in Fig. 6, the split ends of resonator 4 on the right was deliberately separated apart as can be seen in Fig. 7(b). This has been found to have contributed 2 dB to the improvement in isolation. The simulated and measured results of the modified FPD are given in Fig. 10. The fabrication tolerance as well as unaccounted parasitic from the lumped resistor may be the main contributor to the frequency shift.

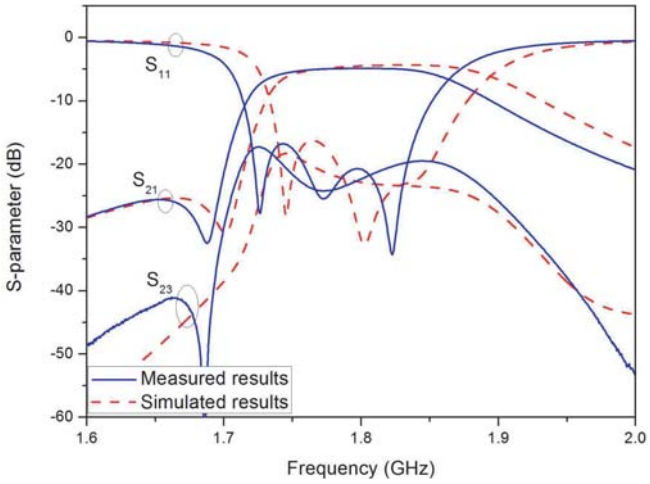

Figure 10. Measured responses of the modified FPD with improved isolation, in comparison with the simulations.

4. CONCLUSIONS

This paper presented a compact and novel coupling structure based on coupled resonators that can be applied to both diplexers and filtering power dividers. Two CT-like structures with two shared resonators were used to generate two transmission zeros while minimising the number of resonators required in the diplexers. These transmission zeros can be adjusted over a wide frequency range by controlling the cross couplings to meet different requirement in rejection and isolation between the channels. The device concept has been experimentally verified by two microstrip diplexers. The simulation and measurement results, which are in excellent agreement with each other, also correspond well with the calculations from the synthesised coupling matrices. The proposed structure provides a technique which could be used to design diplexers with improved isolation without increasing the number of resonators. This compact four-resonator cluster can also be used as the junction structure in higher order diplexers to control the rejections and isolations.

The same topology also works for filtering power dividers. It contains the minimum number of resonators required to realise the 3rd-order two-way FPD with one asymmetric transmission zero. The coupled-resonator network contains two CT structures to improve the out-of-band rejection in the lower band. The fabricated prototype shows an improved out-of-band rejection from 15 dB to 25 dB at below 1.7 GHz. To improve the isolation performance, the FPD was modified and added with one resistor, which increases the isolation from 7 dB to 18 dB across the band.

ACKNOWLEDGMENT

This work was supported by the UK EPSRC under contract EP/M013529/1.

REFERENCES

1. Chuang, M. L. and M. T. Wu, "Microstrip diplexer design using common T-shaped resonator," *IEEE Microw. Wireless Compon. Lett.*, Vol. 21, 583–585, 2011.
2. Cameron, R. J. and M. Yu, "Design of manifold-coupled multiplexers," *IEEE Microw. Mag.*, Vol. 8, 46–59, 2007.
3. Wang, Y. and M. J. Lancaster, "An investigation on the coupling characteristics of a novel multiplexer configuration," *Eur. Microw. Conf.*, 900–903, 2013.
4. Shang, X. B., Y. Wang, W. Xia, et al., "Novel multiplexer topologies based on all-resonator structures," *IEEE Trans. Microw. Theory Tech.*, Vol. 61, 3838–3845, 2013.

5. Macchiarella, G. and S. Tamiazzo, "Synthesis of star-junction multiplexers," *IEEE Trans. Microw. Theory Tech.*, Vol. 58, 3732–3741, 2010.
6. Chuang, M. L. and M.-T. Wu, "Microstrip diplexer design using common T-shaped resonator," *IEEE Microw. Wireless Compon. Lett.*, Vol. 21, 583–585, 2011.
7. Wang, X., J. Wang, and G. Zhang, "Design of wideband filtering power divider with high selectivity and good isolation," *Electron. Lett.*, Vol. 52, 1389–1391, 2016.
8. Shao, J. Y., S. C. Huang, and Y. H. Pang, "Wilkinson power divider incorporating quasi-elliptic filters for improved out-of-band rejection," *Electron. Lett.*, Vol. 47, 1288–1289, 2011.
9. Chen, C. F., T. Y. Huang, T. M. Shen, et al., "Design of miniaturized filtering power dividers for system-in-a-package," *IEEE Trans. Compon. Packag. Technol.*, Vol. 3, 1663–1672, 2013.
10. Li, Q., Y. Zhang, and Y. Fan, "Dual-band in-phase filtering power dividers integrated with stub-loaded resonators," *IET Microw. Anten. Propag.*, Vol. 9, 695–699, 2015.
11. Li, Y. C., Q. Xue, and X. Y. Zhang, "Single- and dual-band power dividers integrated with bandpass filters," *IEEE Trans. Microw. Theory Tech.*, Vol. 61, 69–76, 2013.
12. Avrillon, S., I. Pele, A. Chousseaud, et al., "Dual-band power divider based on semiloop stepped-impedance resonators," *IEEE Trans. Microw. Theory Tech.*, Vol. 51, 1269–1273, 2003.
13. Uchida, H., N. Yoneda, Y. Konishi, et al., "Bandpass directional couplers with electromagnetically-coupled resonators," *2006 IEEE MTT-S Int. Microw. Symp. Digest*, 1563–1566, 2006.
14. Scardelletti, M. C., G. E. Ponchak, and T. M. Weller, "Miniaturized Wilkinson power dividers utilizing capacitive loading," *IEEE Microw. Wireless Compon. Lett.*, Vol. 12, 6–8, 2002.
15. Mirzavand, R., M. M. Honari, A. Abdipour, et al., "Compact microstrip wilkinson power dividers with harmonic suppression and arbitrary power division ratios," *IEEE Trans. Microw. Theory Tech.*, Vol. 61, 61–68, 2013.
16. Miao, C., J. Yang, G. Tian, X. Zheng, et al., "Novel sub-miniaturized wilkinson power divider based on small phase delay," *IEEE Microw. Wireless Compon. Lett.*, Vol. 24, 662–664, 2014.
17. Yu, X. and S. Sun, "Synthesis of filtering power divider with complex source and load impedances," *2016 IEEE Int. Symp. Antennas and Propagation (APSURSI)*, 1719–1720, 2016.
18. Skaik, T. F., M. J. Lancaster, and F. Huang, "Synthesis of multiple output coupled resonator circuits using coupling matrix optimisation," *IET Microw. Antennas Propag.*, Vol. 5, 1081–1088, 2011.
19. Deng, Y., J. Wang, L. Zhu, et al., "Filtering power divider with good isolation performance and harmonic suppression," *IEEE Microw. Wireless Compon. Lett.*, Vol. 26, 984–986, 2016.
20. Chen, C. F. and C. Y. Lin, "Compact microstrip filtering power dividers with good in-band isolation performance," *IEEE Microw. Wireless Compon. Lett.*, Vol. 24, 17–19, 2014.
21. Hong, J. S. and M. J. Lancaster, "Microstrip cross-coupled trisection bandpass filters with asymmetric frequency characteristics," *Proc. Inst. Elect. Eng.*, Vol. 146, 84–90, 1999.
22. Zhang, X. Y., K. X. Wang, and B. J. Hu, "Compact filtering power divider with enhanced second-harmonic suppression," *IEEE Microw. Wireless Compon. Lett.*, Vol. 23, 483–485, 2013.
23. Hong, J. S. and M. J. Lancaster, *Microstrip Filters for RF/Microwave Applications*, Wiley, 2001.